



# Identification of candidate genes associated with resistance to aflatoxin production in peanut through genetic mapping and transcriptome analysis

Dongxin Huai<sup>1</sup> · Li Huang<sup>1</sup> · Xiaomeng Xue<sup>1</sup> · Bolun Yu<sup>1</sup> · Yingbin Ding<sup>1</sup> · Gaorui Jin<sup>1</sup> · Hao Liu<sup>2</sup> · Manish K. Pandey<sup>3</sup> · Hari Kishan Sudini<sup>3</sup> · Huaiyong Luo<sup>1</sup> · Xiaojing Zhou<sup>1</sup> · Nian Liu<sup>1</sup> · Weigang Chen<sup>1</sup> · Liying Yan<sup>1</sup> · Yuning Chen<sup>1</sup> · Xin Wang<sup>1</sup> · Qianqian Wang<sup>1</sup> · Yanping Kang<sup>1</sup> · Zhihui Wang<sup>1</sup> · Xiaoping Chen<sup>2</sup> · Huifang Jiang<sup>1</sup> · Yong Lei<sup>1</sup> · Boshou Liao<sup>1</sup>

Received: 13 August 2024 / Accepted: 15 January 2025 / Published online: 13 March 2025  
© The Author(s), under exclusive licence to Springer-Verlag GmbH Germany, part of Springer Nature 2025

## Abstract

**Key message** Two major QTLs *qAftA07* and *qAftB06.2* for peanut aflatoxin production resistance were identified and candidate genes for them were predicted.

**Abstract** Peanut (*Arachis hypogaea* L.) is a globally significant oil and economic crop, serving as a primary source of edible oil and protein. Aflatoxin contamination is a main risk factor for peanut food safety and industry development worldwide. The most cost-economic and effective control strategy entails the exploration and utilization of natural resistance in peanut, alongside the development of resistant varieties. However, the underlying mechanism of resistance to aflatoxin production (AP) in peanuts remains elusive. In this study, a RIL population derived from a cross between Zhonghua 10 (susceptible) and ICG 12625 (resistant), was used to identify quantitative trait loci (QTLs) for AP resistance. Overall, seven QTLs associated with AP resistance were mapped on five chromosomes, explaining 6.83–17.86% of phenotypic variance (PVE). Notably, only two major QTLs, namely *qAftA07* and *qAftB06.2*, were consistently detected across different environments with 6.83–16.52% PVE. To predict the candidate genes for AP resistance in *qAftA07* and *qAftB06.2*, the transcriptome analysis of seeds from parental lines inoculated with *Aspergillus flavus* were conducted. A total of 175 and 238 candidate genes were respectively identified in *qAftA07* and *qAftB06.2*, encompassing genes with non-synonymous genomic variations as well as differentially expressed genes. Combined with the weighted gene co-expression network analysis, 10 and 11 genes in *qAftA07* and *qAftB06.2* were characterized showing a high correlation with aflatoxin content, thereby representing the most promising candidate genes within these two QTLs. These results provide valuable insights for future map-based cloning studies targeting candidate genes associated with AP resistance in peanut.

---

Communicated by Rod Snowdon.

---

Dongxin Huai and Li Huang have contributed equally to this work.

---

✉ Yong Lei  
leiyong@caas.cn

✉ Boshou Liao  
lboshou@hotmail.com

Institute, Guangdong Academy of Agricultural Sciences,  
Guangzhou, China

<sup>3</sup> International Crops Research Institute for the Semi-Arid  
Tropics (ICRISAT), Hyderabad, Telangana, India

<sup>1</sup> Key Laboratory of Biology and Genetic Improvement of Oil Crops, Ministry of Agriculture and Rural Affairs, Oil Crops Research Institute of Chinese Academy of Agricultural Sciences, Wuhan, China

<sup>2</sup> Guangdong Provincial Key Laboratory of Crop Genetic Improvement, South China Peanut Sub-Center of National Center of Oilseed Crops Improvement, Crops Research

## Introduction

Peanut (*Arachis hypogaea* L.) is a globally significant crop, not only for its economic importance in vegetable oil production but also as a valuable source of protein, calcium, iron, and various vitamins (Mingrou et al. 2022). It is widely grown in the semi-arid tropics, often on marginal soils with limited inputs, and usually intercropped with cereals in many of the developing countries (Feng et al. 2021). Given its nutritional value, peanut cultivation plays a great role in alleviating hunger and addressing malnutrition in these nations.

Aflatoxin contamination is a significant threat to both peanut industry and food safety, as aflatoxin is a highly toxic, carcinogenic, and teratogenic mycotoxin produced by *Aspergillus flavus* and *A. parasiticus* (Alameri et al. 2023). Aflatoxin contamination in peanut occurs throughout the pre-harvest, during-harvest, and post-harvest, primarily during drying, storage and transportation processes (Jallow et al. 2021). Diverse prevention strategies for aflatoxin contamination have been implemented worldwide, including biological, chemical, and physical management practices (Shabeer et al. 2022). Among them, the development and cultivation of peanut varieties exhibiting suitable resistance to *A. flavus* infection and/or aflatoxin production is considered as the most efficacious and cost-effective approach (Soni et al. 2020a). Therefore, the exploration and utilization of the resistance in peanut has become the main control strategy of aflatoxin contamination.

The resistance to aflatoxin contamination in peanut consists of three components or mechanisms including: a) shell infection resistance, b) seed infection resistance, and c) aflatoxin production (AP) resistance (Ding et al. 2022). The inheritance of these three resistances was found to be independent from each other, and they were controlled by distinct genes exhibiting additive effects. (Ding et al. 2022; Torres et al. 2014; Yu et al. 2019). Quantitative trait loci (QTLs) for shell infection resistance were detected on chromosomes A01, B02 and B10 with 26.99–38.64% phenotypic variance explained (PVE) (Ding et al. 2022). The QTLs for seed infection resistance were identified on chromosomes A03, A04, A05, A08, A10, B01, B03, B04 and B10 with 5.15–19.00% PVE (Jiang et al. 2021; Khan et al. 2020; Yu et al. 2019). The QTLs for AP resistance were predominantly mapped to A05, A07 and B06 chromosomes with 4.61–21.02% (Jin et al. 2023; Yu et al. 2019, 2020, 2024). In recent years, significant progress has been made in identifying several QTLs associated with peanut AP resistance. However, there still exists a deficiency in the exploration of resistance genes and mechanism analysis, which hinders the breeding progress towards resistant peanut cultivars.

Omics approaches have been employed in the investigation of mechanisms underlying resistance to aflatoxin

contamination in peanut. Transcriptome analyses of seeds inoculated with *A. flavus* from resistant and susceptible genotypes revealed that disease resistance, hormone biosynthetic signaling, reactive oxygen species (ROS) detoxification, cell wall metabolism and catabolism, flavonoid, stilbenoid, and phenylpropanoid biosynthesis pathways, as well as seed germination pathways were associated with resistance to aflatoxin production in peanut (Soni et al. 2020b, 2021; Wang et al. 2016). Weighted gene co-expression network analysis (WGCNA) demonstrated that genes encoding pathogenesis-related proteins (PR10), 1-aminocyclopropane-1-carboxylate oxidase (ACO1), MAPK kinase, serine/threonine kinase (STK), pattern recognition receptors (PRRs), cytochrome P450, SNARE protein SYP121, pectinesterase, phosphatidylinositol transfer protein, and pentatricopeptide repeat (PPR) protein play major and active roles in peanut resistance to *A. flavus* (Chai et al. 2024; Cui et al. 2022; Zhao et al. 2024a). Similarly, proteomic analyses have also reported that proteins associated with phenylalanine ammonia lyase, cinnamic acid-4-hydroxylase, chalcone synthase, resveratrol synthase, flavanone-3-hydroxylase, lipoxygenase, diacylglycerolglycerol-3-phosphate-3-phosphatidyltransferase,  $\beta$ -ketoacyl-ACP-reductase, monoacylglycerol acyltransferase, and diacylglycerol acyltransferase were involved in peanut resistance to aflatoxin contamination (Bhatnagar-Mathur et al. 2021). Metabolism analyses found that the involvement of second metabolites, including resveratrol, cinnamic acid, coumaric acid, ferulic acid, pipercolic acid and 13S-HPODE, in conferring peanut resistance to aflatoxin contamination (Sharma et al. 2021; Wang et al. 2023). Omics analyses have facilitated better understanding of the resistance mechanisms and identified pathways involved in peanut resistance to aflatoxin contamination, suggesting that integration of omics analyses with genetic mapping would expedite the elucidation of resistance genes and their underlying mechanisms.

In our previous study, ICG 12625 was identified as exhibiting AP resistance, and a recombinant inbred line (RIL) population was developed through crossing it with the susceptible peanut variety Zhonghua10. Four major QTLs for resistance to AFB<sub>1</sub> and AFB<sub>2</sub> were identified using a linkage map constructed with SSR and transposon markers (Yu et al. 2019). Considering the uneven density and unclear physical position of SSR and transposon markers, a high-density genetic linkage map was constructed employing SNP/InDel markers. The new genetic map contained 2700 bin blocks assigning to 20 linkage groups (LGs) and covered 1469.6 cM genetic distance. The density of genetic map was 1.85 bins/cM and the average bin interval ranged from 0.48 cM to 0.64 cM on each linkage group (Li et al. 2023). In present study, the phenotypic data on aflatoxin contents (AFB<sub>1</sub> + AFB<sub>2</sub>) of 140 individuals were collected

in three consecutive years via inoculation with *A. flavus* in laboratory. QTLs for AP resistance identified, and the transcriptome of seeds from parental lines inoculated with *A. flavus* was investigated. Then the results were combined to predict the candidate genes for peanut AP resistance. The results would contribute to elucidating the genetic basis of resistance to aflatoxin contamination in peanut.

## Materials and methods

### Plant materials

A RIL population ( $F_0$ – $F_{11}$  generation) consisted of 140 lines used in this study was derived from a cross between Zhonghua 10 and ICG 12625. The female parent Zhonghua 10 (*A. hypogaea* var. *vulgaris*) is a susceptible variety to aflatoxin contamination, which was developed by Oil Crops Research Institute of Chinese Academy of Agricultural Science (OCRI-CAAS), Wuhan, China. The male parent ICG 12625 (PI 497597, *A. hypogaea* var. *aequatoriana*) contains resistance to both aflatoxin contamination and bacterial wilt, which was obtained from the International Crop Research Institute for the Semi-Arid Tropics (ICRISAT), Hyderabad, India.

The RIL population and the two parents were planted in experimental field of OCRI-CAAS in Wuhan, China. A random block design with three replications was employed consecutively from 2018 to 2020. Each plot consisted a single row containing 10–12 plants, spaced at intervals of 10 cm within each row and 30 cm between rows. Field management followed the standard agricultural practices.

### Phenotyping for aflatoxin content

The toxicogenic *A. flavus* strain (AF2202) was used for evaluation of peanut resistance to aflatoxin contamination. Conidia of AF2202 were cultured on fresh potato dextrose agar medium at  $29 \pm 1$  °C for 7 days, and then collected and suspended in sterile water containing 0.05% Tween-80. The concentration of conidia in the suspension was determined using a haemocytometer. Approximately 20 g of healthy and mature peanut seeds harvested from each line in a single year were carefully selected, followed by surface sterilization using 75% ethanol for 1 min. The seeds were then rinsed three times with sterile distilled water. Then, the seeds were immersed in 1 ml of *A. flavus* conidial suspension ( $2 \times 10^6$  conidia/ml) in a sterile Petri plate. The plates were incubated in darkness at a temperature of  $29 \pm 1$  °C for 7 days.

The inoculated peanut seeds were rinsed with 75% ethanol to eliminate conidia of *A. flavus* on the seed surface, and then dried at 110 °C for 60 min. Aflatoxin in these seeds were extracted using a 55% ethanol solution and quantified

via an Agilent 1200 high-performance liquid chromatography (HPLC) for aflatoxin content (AFB<sub>1</sub> and AFB<sub>2</sub>) determination. Chromatographic separation was achieved with the C18 column (4.6 mm × 250 mm, 5 μm, Agilent) and methanol–water (45:55) as the mobile phase at a flow rate of 0.7 mL/min.

### Statistical analysis

Statistical analyses for the phenotypic data were performed with IBM SPSS Statistics 20.0 statistical software. The distribution of phenotypes was performed on Origin 2022 software. The broad-sense heritability of aflatoxin content was calculated as  $H^2 = V_g / (V_g + V_{ge}/n + V_e/rn)$ , where  $V_g$  is the genetic variance component,  $V_{ge}$  is the genotype-environment interaction variance component,  $V_e$  is the residual (error) variance component, and  $n$  and  $r$  were defined as the number of environments and the number of replicates, respectively.

### QTL mapping

The genetic linkage map of 140 RILs consisting of 2700 bin blocks and spanning a total genetic distance of 1469.6 cM, was previously constructed (Li et al. 2023).

The QTL mapping was conducted by composite interval mapping method in the Windows QTL Cartographer 2.5 software, using the mean value in each environment (Basten et al. 2002). The walk speed was set at 1 cM, and the logarithm of the odds (LOD) threshold was set at 2.5. The QTLs were designated using an abbreviated trait name along with the corresponding chromosome number.

### RNA-seq and data processing

Seeds from two parent lines, Zhonghua 10 and ICG 12625, were inoculated with *A. flavus* cultured for 0, 0.5, 1, 3 and 7 days and sampled for RNA isolation and cDNA library construction. Total RNA was extracted following the manufacturer's instructions using TRIzol reagent (DP 424, TIAN-GEN, China). Thirty cDNA libraries were constructed and sequenced using the Illumina HiSeq platform. The raw reads were subjected to filtering and trimming using Trimmomatic (Bolger et al. 2014). The clean reads were aligned to the Tifrunner\_V20190521 version of cultivated peanut reference genome (<https://www.peanutbase.org/>) (Bertioli et al. 2019) using HISAT2 software (Kim et al. 2019). The gene expression abundance values were calculated as Transcripts Per Million mapped reads (TPM) using RSEM (v1.2.31) (Li and Dewey 2011). Differentially expressed genes (DEGs) were identified by DESeq2 (v1.10.1) (Love et al. 2014), considering a  $TPM \geq 1$  in at least one sample ( $\log_2$  fold change  $\geq 1$  and  $FDR < 0.05$ ). Venn diagrams, correlation

heatmaps, and gene expression heatmaps were generated with TBtools (Chen et al. 2020). Gene Ontology (GO) and Kyoto Encyclopedia of Genes and Genomes (KEGG) enrichment analysis was performed using the R function phyper (Consortium 2019; Kanehisa et al. 2017). The co-expression network analysis was conducted with the WGCNA package in R (Langfelder and Horvath 2008).

### Candidate genes analysis

The functions of polymorphic loci including SNPs and InDels were performed using the SnpEff v3.0 software (Cingolani et al. 2012). The putative genes affected by non-synonymous SNPs in the major QTL were selected as potential candidates for AP resistance. Additionally, DEGs located within the major QTL regions were also considered as promising candidates for AP resistance. The functions of candidate genes were predicted using the Mapman tools (v3.6.0R1) (Thimm et al. 2004).

## Results

### Phenotypic variation of aflatoxin production resistance

The resistance performance of two parents and the RIL population was investigated by artificial inoculation with toxicogenic *A. flavus* in laboratory. Significant difference of aflatoxin content between Zhonghua 10 and ICG 12625 were observed across three different environments. The resistance of ICG 12625 to aflatoxin accumulation was found to be superior compared to Zhonghua 10 (Table 1). The RIL population exhibited transgressive segregation and a continuous distribution of aflatoxin content across all environments (Fig. 1A). The aflatoxin content of RILs ranged from 59.84 to 360.07  $\mu\text{g/g}$  in the 2018 environment, from 66.20 to 278.07  $\mu\text{g/g}$  in the 2019 environment, from 47.87 to 254.58  $\mu\text{g/g}$  in the 2020 environment (Table 1). Broad-sense heritability for aflatoxin content was estimated to be 0.77 (Table 1), indicating that AP resistance was controlled by genetic factors.

### Detection of QTLs for aflatoxin production resistance

The QTL mapping for peanut AP resistance was conducted using the high-density genetic map (Li et al. 2023) and the phenotypic data of aflatoxin content obtained from the RILs during 2018–2020 in Wuhan. A total of seven QTLs associated with AP resistance were identified in the three environments explaining 6.83–17.86% of phenotype variation (Table 2). These QTLs were mapped onto five chromosomes, comprising three chromosomes of the A sub-genome and two chromosomes of the B sub-genome (Table 2). Three QTLs were identified onto chromosome B06, and one QTL each was mapped onto A01, A07, A10 and B07 (Table 2).

The two major QTLs, *qAftA07* and *qAftB06.2*, were detected in multiple environments within the same genomic region, exhibiting PVE ranges of 6.83% to 10.10% and 15.66% to 16.52%, respectively (Table 2; Fig. 1B). The *qAftA07* locus spanned a physical region of 0.00–3.60 Mb on A07 chromosome, where the *qAftB06.2* locus occupied a range of 9.24–21.75 Mb on B06 chromosome (Table 2). Another two major QTLs, *qAftB06.1* and *qAftB06.3*, were also located on B06 chromosome accounting for 17.86% and 13.55% PVE, respectively; however, their presence was limited to a single environment (Table 2). Minor QTLs namely, *qAftA01*, *qAftA10* and *qAftB07* with a PVE of 7.29%, 7.69% and 7.57% respectively, were solely detected in a single environment (Table 2).

The effects of the two major QTLs *qAftA07* and *qAftB06.2*, were evaluated by utilizing genotypes of c07b010 (CI: 6.7 cM) and c16b043 (CI: 27.4 cM) bin blocks, which were positioned closet to the peaks of QTLs (Table 2; Fig. 1B). The genotypes of c07b010 and c16b043 derived from Zhonghua 10 were designated as “A1A1” and “B1B1”, while the genotypes from ICG 12625 were designated as “A2A2” and “B2B2”, respectively. As shown in Fig. 1C, the aflatoxin contents in seeds with genotype “A1A1” were significantly lower than those in seeds with genotype “A2A2” in both the 2019 and 2020 environments. Conversely, the aflatoxin contents in seeds with genotype “B1B1” were significantly higher than those in seeds with genotype “B2B2” across all the three environments (Fig. 1C). These results suggest that both

**Table 1** The phenotypic variation of aflatoxin content in the RIL population

Env	Parents ( $\mu\text{g/g}$ )		RILs ( $\mu\text{g/g}$ )		CV	H <sup>2</sup>
	Zhonghua 10	ICG 12625	Range	Mean $\pm$ SD		
2018	191.70 $\pm$ 35.58	91.79 $\pm$ 11.25**	59.84–360.07	180.51 $\pm$ 88.45	0.49	0.77
2019	161.39 $\pm$ 17.42	84.15 $\pm$ 5.02**	66.20–278.07	148.36 $\pm$ 57.86	0.39	
2020	148.21 $\pm$ 17.74	92.64 $\pm$ 17.92**	47.87–254.58	127.52 $\pm$ 65.04	0.51	

Env environment, SD standard deviation, CV coefficient of variation

\*\*Difference is significant at  $p < 0.01$  level between parents

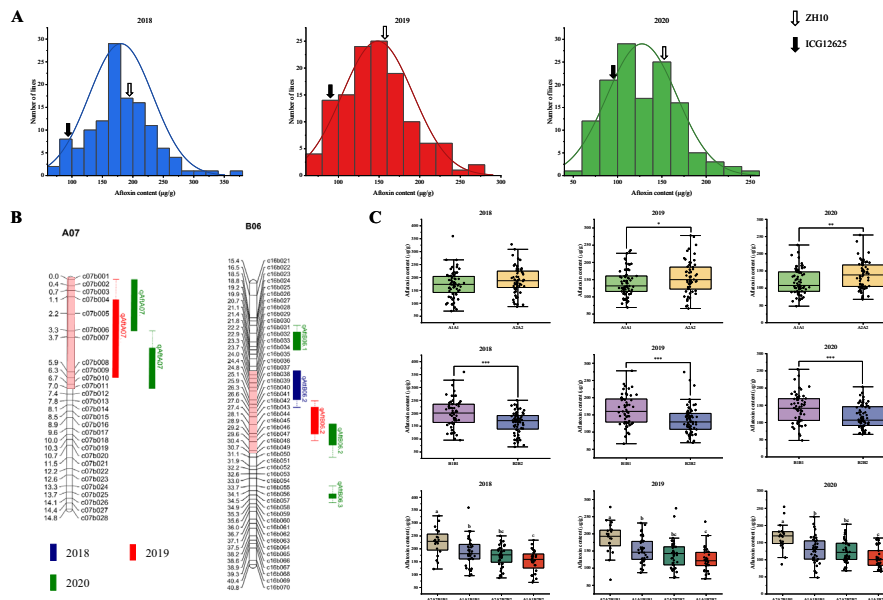


**Fig. 1** Phenotypic variation and QTL mapping for peanut aflatoxin production resistance. **A** Phenotypic distribution of aflatoxin content in the RIL population derived from the cross between Zhonghua 10 and ICG 12625. **B** Distribution of QTLs for peanut aflatoxin production resistance on A07 and B06 chromosomes. **C** Phenotypic effect of the major QTLs *qAftA07* and *qAftB06.2*. The alleles of

*qAftA07* and *qAftB06.2* derived from Zhonghua 10 were designated as “A1A1” and “B1B1”, while the alleles from ICG 12625 were designated as “A2A2” and “B2B2”, respectively. \* $p < 0.05$ ; \*\* $p < 0.01$ ; \*\*\* $p < 0.001$ . a, b and c represent significant difference at  $p < 0.05$  based on ANOVA and Fisher’s least significant difference (LSD) multiple-comparison

**Table 2** The genomic region for aflatoxin content identified by QTL mapping

QTL	Chr	Env	Position (cM)	CI (cM)	Physical interval (Mb)	LOD	PVE (%)	Add
<i>qAftA01</i>	A01	2020	79.21	78.1–82.9	106.06–107.22	3.16	7.29	1.08
<b><i>qAftA07</i></b>	A07	2019	3.31	0.0–6.3	0.00–3.45	3.16	6.83	–1.18
		2020	1.11	0.0–3.3	0.00–2.80	3.12	7.55	–1.11
		2020	6.71	3.3–7.0	2.78–3.60	4.24	10.10	–1.29
<i>qAftA10</i>	A10	2019	3.81	0.0–4.2	0.00–1.86	4.03	7.69	1.23
<i>qAftB06.1</i>	B06	2020	21.11	19.2–21.4	7.74–9.04	7.17	17.86	1.70
<b><i>qAftB06.2</i></b>	B06	2018	23.71	23.3–26.6	9.24–20.76	5.92	15.67	2.16
		2019	27.41	26.0–29.6	13.32–20.76	6.84	15.66	1.83
		2020	28.91	28.1–31.1	14.93–21.75	6.57	16.52	1.67
<i>qAftB06.3</i>	B06	2020	34.51	33.7–35.2	23.15–29.97	5.27	13.55	1.49
<i>qAftB07</i>	B07	2019	44.81	42.5–47.4	123.95–127.29	3.46	7.57	1.23

QTLs identified in more than one environment are highlighted in bold

Chr chromosome, Env environment, CI confidence interval of QTLs, PVE phenotypic variance explained, Add additive effect

the parents possess favorable alleles for AP resistance. Hence, the combined effect of *qAftA07* and *qAftB06.2* was assessed. The seeds with genotype “A1A1B2B2” accumulated lowest aflatoxin contents compared to seeds with other genotypes (A2A2B1B1, A1A1B1B1 and A2A2B2B2) across all the three environments (Fig. 1C), indicating that the introgression of favorable alleles from both *qAftA07* and *qAftB06.2* could enhance resistance to aflatoxin accumulation.

### Identification of DEGs associated with aflatoxin production resistance

To identify differently expressed genes (DEGs) associated with peanut AP resistance, RNA-seq analysis of seeds inoculated with *A. flavus* from two parents Zhonghua 10 and ICG 12625 was performed. Samples were collected at 0, 0.5, 1, 3, 7 days after inoculation (DAI) from the infected seeds of Zhonghua 10 and ICG 12625. As shown in Fig. 2A, no

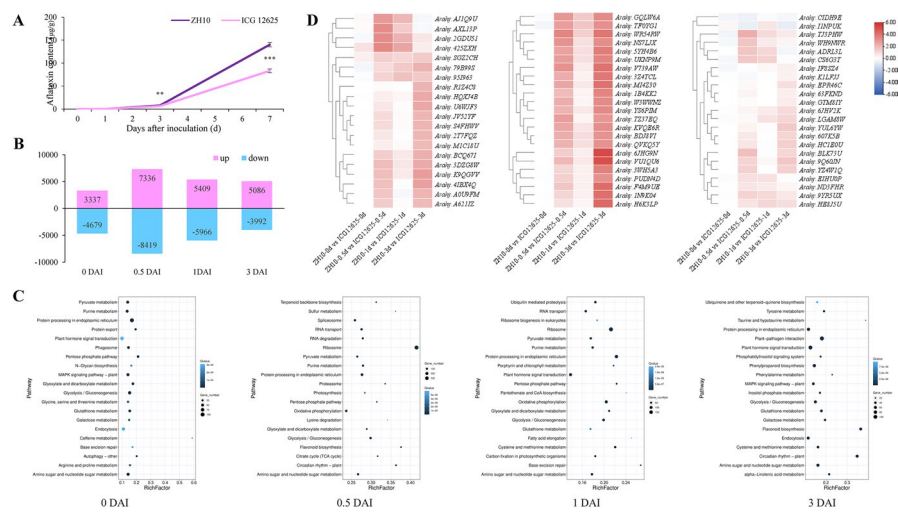


**Fig. 2** Analysis of aflatoxin levels and transcriptome profiles in seeds inoculated with *A. flavus* strains from Zhonghua 10 (ZH10) and ICG 12625. **A** Aflatoxin contents in seeds collected at 0, 0.5, 1, 3 and 7 days after inoculation (DAI).  $**p < 0.01$ ;  $***p < 0.001$ . **B** The number of upregulated (upper bars) and downregulated (lower bars) genes in ICG 12615 as compared with Zhonghua 10 at each stage of seed

infection. **C** Enriched KEGG pathways of DEGs between Zhonghua 10 and ICG 12625 at each stage of seed infection. **D** Heat map of DEGs involved in the flavonoid biosynthesis pathway. The color indicates the log<sub>2</sub>fold-change of gene expression value in ICG 12625 to that in Zhonghua 10 at the same infection stage

aflatoxin was detected in seeds of both Zhonghua 10 and ICG 12625 at 0, 0.5 and 1 DAI. The aflatoxin content in Zhonghua 10 detected at 3 DAI was significantly higher than that in ICG 12625 (7.85 µg/g vs. 6.37 µg/g). At 7 DAI, the aflatoxin content in Zhonghua 10 increased to a remarkably high level of 140.25 µg/g, where it only reached 83.16 µg/g in ICG 12625. These results indicated that the AP resistance of ICG 12625 was consistently higher than that of Zhonghua 10.

A total of 264.13 Gb of high-quality data from 30 samples, with each sample yielding clean data amounting to 8.80 Gb. On average, 84.01% of reads were successfully aligned to the peanut reference genome, except for samples collected at 7 DAI. The average alignment rates of Zhonghua 10 and ICG 12625 at 7 DAI were 7.53% and 11.99%, respectively (Table S1), due to a higher presence of mycelium and spores in kernels from seeds collected at this time point, resulting in a majority of reads mapping to the *A. flavus* genome. Therefore, data from samples collected at 7 DAI were excluded, while data from samples collected at 0, 0.5, 1 and 3 DAI were utilized for subsequent analysis.

In seeds inoculated with *A. flavus* of Zhonghua 10 and ICG 12625, a total of 53,476 and 55,188 genes were identified and found expressed. Among them, 50,880 genes were detected in both parents, while 2596 and 4308 genes were specifically expressed in Zhonghua 10 and ICG 12625 (Fig. S1A). In total, 25,649 DEGs were identified in peanut during infection of *A. flavus*. In Zhonghua 10, a total of 3157 genes were found to be up-regulated in the first half-day period, while 3056 genes were down-regulated.

Subsequently, during the following half-day period, there was an up-regulation of 2540 genes and a down-regulation of 2090 genes. Furthermore, over the course of the subsequent two days, there was an up-regulation of 3242 genes and a down-regulation of 3999 genes (Fig. S1B). Comparatively in ICG 12625, more genes were induced with a total count of 10,309 up-regulated and 7852 down-regulated during the initial half-day period. However fewer gene inductions occurred in ICG 12625 during the following days with only counts of 1728 and 1,680 for up- and down-regulated respectively within the subsequent half-day period; whereas within the subsequent two days counts reached only at levels of 2067 for up-regulated and 541 for down-regulated (Fig. S1B). In comparison to Zhonghua 10, ICG 12625 exhibited up-regulation of 3337, 7336, 5409 and 5086 genes at 0, 0.5, 1 and 3 DAI respectively; whereas down-regulation was observed in the expression of 4679, 8419, 5966 and 3992 genes at the corresponding time points (Fig. 2B). GO analysis of these DEG genes primarily enriched in the cellular components, including vacuole, plastid, peroxisome, nucleoplasm, nucleolus, nuclear envelope, mitochondrion, lysosome, Golgi apparatus, endosome, endoplasmic reticulum, cytosol, chloroplast; the molecular functions encompassing signaling receptor binding, RNA binding, DNA binding, nuclease activity, kinase activity; and the biological process including translation, signal transduction, post-embryonic development and cellular protein modification process (Fig. S1C).

KEGG pathway analysis was performed to reveal the metabolic mechanisms involved in peanut AP resistance.

The Zhonghua 10 dataset demonstrated a significant enrichment of 128 pathways, with 120 pathways being commonly enriched throughout the entire infection process (Fig. S1D). In contrast, the ICG 12625 dataset also showed a significant enrichment of 128 pathways; however, only 54 pathways exhibited consistent enrichment throughout the entire infection process, while an additional 66 pathways displayed specific enrichment on the first day of infection (Fig. S1E). A total of 123 pathways were significantly enriched throughout the entire infection process in both of Zhonghua 10 and ICG 12625 (Fig. S1F), including plant hormone signal transduction, plant-pathogen interaction, oxidative phosphorylation, flavonoid biosynthesis, isoflavonoid biosynthesis, phenylpropanoid biosynthesis, sulfur metabolism, glutathione metabolism and alpha-linolenic acid metabolism (Fig. 2C). Although ICG 12625 demonstrated a greater induction of genes and a more rapid response compared to Zhonghua 10 during *A. flavus* infection, the pathways implicated in their resistance against AP remained consistent. The difference between them is that the number of induced genes was higher in ICG 12625 after inoculation with *A. flavus* compared to Zhonghua 10, along with a greater fold-change. For example, in the flavonoid biosynthesis pathway, Zhonghua 10 exhibited regulation of 43 genes, whereas ICG 12625 showed regulation of 61 genes. Moreover, the expression levels of 65 genes in ICG 12625 were higher than them in Zhonghua 10, while only one gene displayed a lower expression level. (Fig. 2D).

## Exploration of key modules associated with aflatoxin production resistance

To explore key genes that were highly associated with peanut AP resistance, the DEGs were used to perform WGCNA after filtering. As a result, a scale-free network with 15 co-expression modules was constructed (Fig. 3A). The number of genes among 15 modules ranged from 97 to 16,683.

To characterize the key modules associated with AP resistance in peanut seeds, the module-trait relationships (MTRs) were analyzed. As shown in Fig. 3B, the black ( $r=0.77$ ,  $p<0.001$ ), salmon ( $r=0.51$ ,  $p<0.05$ ) and yellow ( $r=0.42$ ,  $p<0.05$ ) modules were significantly positively correlated with aflatoxin content, while the blue ( $r=-0.42$ ,  $p<0.05$ ) was significantly negatively correlated with aflatoxin content.

A total of 770 genes were identified in the black module, exhibiting significant enrichment in GO terms related to DNA binding, plastid, cytosol, mitochondrion, and chloroplast (Fig. 3C). Within the black module, 14 genes were found to be involved in the oxidative phosphorylation pathway, 10 genes were associated with plant hormone signal transduction pathway, and 8 genes participated in phenylpropanoid biosynthesis pathway (Fig. S2A). The salmon module consisted of 97 genes, demonstrating significant enrichment in a single GO term related to DNA binding. Within the salmon module, most genes were found to be involved in pathways related to amino acid metabolism (Fig. S2B). There were 1435 genes in the yellow module, which demonstrated significant enrichment in the same GO terms as the black module (Fig. 3C). Within the yellow module, 40 genes

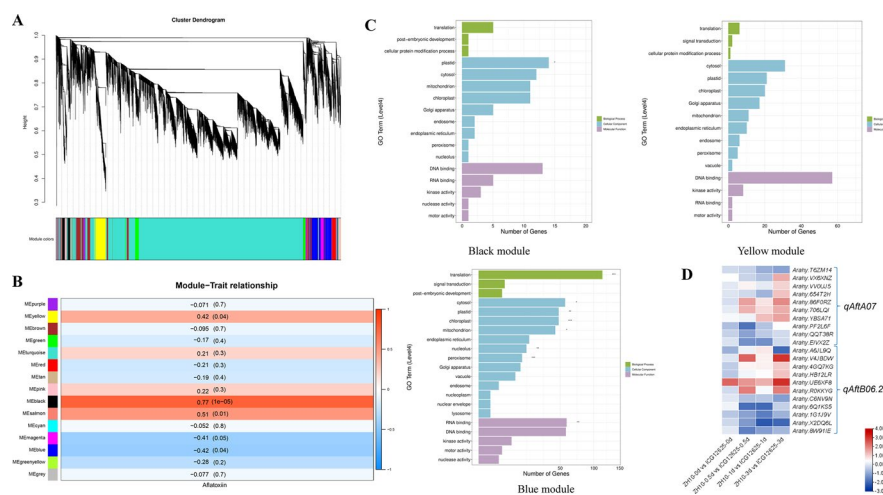


**Fig. 3** The WGCNA analysis and candidate gene prediction for peanut aflatoxin production resistance. **A** Hierarchical clustering tree (dendrogram) of genes based on co-expression network analysis in Zhonghua 10 and ICG 12625. **B** Correlation analysis between co-expression modules and aflatoxin content. Boxes contained Pearson correlation coefficients and  $p$  values. **C** Enriched functional GO terms

of genes in the co-expression module. GO terms with  $p$ -value  $< 0.05$  were listed in the y-axis. **D** Heat map of predicted candidate genes in *qAflA07* and *qAflB06.2*. The color indicates the log<sub>2</sub> fold-change of gene expression value in ICG 12625 to that in Zhonghua 10 at the same infection stage

were found to be involved in the plant hormone signal transduction pathway, 36 genes were associated with flavonoid biosynthesis, 16 genes participated in alpha-linolenic acid metabolism pathway, and 14 genes were found to be related to glutathione metabolism pathway (Fig. S2C). A total of 2307 genes were identified in the blue module, displaying significant enrichment in GO terms related to translation, plastid, cytosol, mitochondrion, chloroplast, DNA binding and RNA binding (Fig. 3C). Among these genes within the blue module, 27 were found to be implicated in the oxidative phosphorylation pathway while another 15 were linked to plant hormone signal transduction pathway (Fig. S2D). Overall, the genes within the black, salmon, yellow, and blue modules exhibit a strong association with peanut AP resistance; therefore, genes in these four modules deserves more attention in subsequent analysis.

### Candidate gene prediction in major QTLs for aflatoxin production resistance

Totally, 721 SNP and 188 InDels were identified in the candidate region of *qAftA07* (0.00–3.60 Mb on the A07 chromosome). Among them, 377 SNPs and 98 InDels were intergenic, 115 SNPs and 33 InDel were upstream/downstream, and 229 SNPs and 57 InDels were genic (Table 3). There were 431 genes in the candidate region (Table 4; Table S2),

**Table 3** Variations in the candidate region of *qAftA07* and *qAftB06.2*

QTL	Category	SNP	InDel	
<i>qAftA07</i>	Intergenic	377	98	
	Upstream and downstream	115	33	
	Upstream	66	20	
	Downstream	44	10	
	Upstream/downstream	5	3	
	Genic	229	57	
	Intronic	93	26	
	Exonic	116	13	
	UTR5'	6	10	
	UTR3'	13	8	
	Splicing	1	0	
	<i>qAftB06.2</i>	Intergenic	1629	440
		Upstream and downstream	146	69
Upstream		79	35	
Downstream		64	31	
Upstream/downstream		3	3	
Genic		143	67	
Intronic		79	41	
Exonic		47	7	
UTR5'		8	7	
UTR3'		9	11	
Splicing		0	1	

**Table 4** Genes in the candidate region of *qAftA07* and *qAftB06.2*

QTL	Number of genes	Number of expressed genes	Number of genes with nonsynonymous variation	Number of DEGs	Number of candidate gene
<i>qAftA07</i>	413	216	17	168	175
<i>qAftB06.2</i>	618	325	12	235	238

but only 216 of them were expressed in developing seeds (Table 4; Fig. S3A). Of these 216 genes, 17 exhibited nonsynonymous variations (Table 4; Table S4), while 168 genes were identified as DEGs (Table 4; Fig. S4A). In total, a set of 175 candidate genes were identified in *qAftA07* (Table 4).

Based on the integration of key modules associated with peanut AP resistance, a set of 10 genes were identified as highly promising candidate genes, comprising one gene from the black module, six genes from the yellow module, and three genes from the blue module (Table 5). The expression levels of three genes, namely *Arahy.T6ZM14*, *Arahy.QQT38R*, and *Arahy.EIVX2Z*, were consistently down-regulated in ICG12635 compared to those in Zhonghua10 (Fig. 3D). However, the gene *Arahy.PF2L6F* exhibited down-regulation only on the initial first day but not at 3DAI (Fig. 3D). The expression levels of three genes, specifically *Arahy.VX6XNZ*, *Arahy.VV0UJ5* and *Arahy.654T2H* were initially down-regulated but subsequently up-regulated at 3 DAI (Fig. 3D). The expression levels of two genes, *Arahy.86FORZ* and *Arahy.706LQI*, exhibited consistent up-regulation upon inoculation with *A. flavus*, while the expression level of *Arahy.YBSA7I* was observed to be up-regulated from 1 to 3 DAI (Fig. 3D). Six SNPs were identified in *Arahy.VV0UJ5*, and two of them resulted in nonsynonymous variation (Table S6). One SNP was found within the intron of *Arahy.PF2L6F*, and another SNP was found upstream of *Arahy.QQT38R* (Table S6). Therefore, these ten genes were considered as the most promising candidate gene in *qAftA07*.

Totally, 1918 SNP and 576 InDels were identified in the candidate region of *qAftB06.2* (9.24–21.75 Mb on the B07 chromosome). Among them, 1629 SNPs and 440 InDels were intergenic, 146 SNPs and 69 InDel were upstream/downstream, and 143 SNPs and 67 InDels were genic (Table 3). There were 618 genes in the candidate region (Table 4; Table S2), but only 325 of them were expressed in developing seeds (Table 4; Fig. S3B). Of these 325 genes, 12 exhibited nonsynonymous variations (Table S5), while 235 genes were identified as DEGs (Table 4; Fig. S4B). In total, a set of 238 candidate genes were identified in *qAftB06.2* (Table 4).

Similarly, combined with the result of key modules associated with peanut AP resistance, 11 genes were

**Table 5** Candidate genes identified by WGCNA analysis and gene function annotation

QTL	Module	Gene ID	Annotation
<i>qAftA07</i>	Black	<i>Arahy.T6ZM14</i>	Receptor-like protein
	Yellow	<i>Arahy.VX6XNZ</i>	Predicted NUDIX hydrolase FGF-2 and related proteins
		<i>Arahy.VV0UJ5</i>	Cytochrome P450 71D10
		<i>Arahy.654T2H</i>	Scarecrow-like protein 21 isoform X1
		<i>Arahy.86FORZ</i>	Probable serine/threonine-protein kinase WNK11 isoform X1
		<i>Arahy.706LQI</i>	Calcium-dependent protein kinase 2
	Blue	<i>Arahy.YBSA71</i>	Reactive intermediate deaminase A
		<i>Arahy.PF2L6F</i>	Cell division cycle protein 48 homolog
		<i>Arahy.QQT38R</i>	Serine/threonine-protein kinase BSK1
		<i>Arahy.EIVX2Z</i>	ATPase WRNIP1
		<i>Arahy.A6JL9Q</i>	Bifunctional 3-dehydroquinase dehydratase/shikimate dehydrogenase
<i>qAftB06.2</i>	Black	<i>Arahy.A6JL9Q</i>	Bifunctional 3-dehydroquinase dehydratase/shikimate dehydrogenase
	Yellow	<i>Arahy.V4JBDW</i>	Potassium transporter 5
		<i>Arahy.4GQ7KG</i>	Glucose-6-phosphate 1-dehydrogenase 4
		<i>Arahy.HB12LR</i>	F-box protein PP2-B15
		<i>Arahy.UE6XF8</i>	E3 ubiquitin protein ligase DRIP2 isoform X1
		<i>Arahy.R0KKYG</i>	Phosphoenolpyruvate carboxylase kinase 2
	Blue	<i>Arahy.C6NV9N</i>	GATA transcription factor 15
		<i>Arahy.6Q1KS5</i>	S-adenosylmethionine synthase 1
		<i>Arahy.1G1J9V</i>	Dormancy-associated protein homolog 3
		<i>Arahy.X2DQ6L</i>	GPI-anchored protein
		<i>Arahy.8W91IE</i>	Superoxide dismutase

identified as highly promising candidate genes, comprising one gene from the black module, five genes from the yellow module, and five genes from the blue module (Table 5). The expression levels of five genes, namely *Arahy.C6NV9N*, *Arahy.6Q1KS5*, *Arahy.1G1J9V*, *Arahy.X2DQ6L*, and *Arahy.8W91IE*, were consistently down-regulated in ICG12635 compared to those in Zhonghua10 (Fig. 3D). The gene *Arahy.A6JL9Q* displayed a decrease in expression at 0 DAI, followed by an increase at 1 DAI and another decrease at 3 DAI (Fig. 3D). The expression levels of two genes, *Arahy.V4JBDW* and *Arahy.R0KKYG*, were significantly up-regulated at 0.5 DAI and 3 DAI, whereas the expression levels of *Arahy.4GQ7KG* and *Arahy.HB12LR* showed a slight increase from 0.5 DAI to 3 DAI (Fig. 3D). The expression level of *Arahy.UE6XF8* exhibited consistent up-regulation from 0 to 3 DAI (Fig. 3D). A single SNP was identified downstream of *Arahy.A6JL9Q* and *Arahy.V4JBDW* for each, while one InDel was detected downstream of *Arahy.R0KKYG* (Table S6). The upstream region of *Arahy.6Q1KS5* was found to harbor a single SNP, while another SNP was detected within the intron of *Arahy.4GQ7KG* (Table S6). Therefore, these eleven genes were considered as the most promising candidate gene in *qAftB06.2*.

## Discussion

Aflatoxin contamination is a worldwide challenge for both the peanut industry and consumers. Genetic enhancement for aflatoxin resistance is widely considered as the most cost-effective approach to control contamination risk in this crop. The identification of resistant genes and elucidation of the mechanisms underlying resistance to aflatoxin contamination serve as the fundamental basis for peanut breeding programs aimed at enhancing resistance.

### The QTLs *qAftA07* and *qAftB06.2* exhibit stable resistance to peanut aflatoxin production

In this study, two major QTLs associated with peanut AP resistance were identified using the RIL population derived from the cross of Zhonghua 10 and ICG 12625 (Table 2). The two major QTLs *qAftA07* and *qAftB06.2* were mapped to A07 and B06 chromosomes, respectively, which were in accordance with findings reported in the previous study (Yu et al. 2019). The *qAftA07* locus with a 6.83–10.10% PVE was detected in both the 2019 and 2020

environments (Table 2), while the previously reported corresponding QTL with a 10.62–17.87% PVE was detected across the 2013, 2014 and 2015 environments (Yu et al. 2019). The absence of the *qAftA07* locus in 2018 may be attributed to the favorable environmental conditions, which were more suitable to plant growth compared to those in 2019 and 2020. The temperature in 2018 exhibited a moderate trend compared to that of 2019 and 2020 (<http://data.cma.cn>). Additionally, there was no significant variation in soil moisture among the three environments due to the presence of irrigation facilities within the field. Additionally, the *qAftB06.2* locus with a 15.66–16.52% PVE was detected across the 2018, 2019 and 2020 environments (Table 2), while the previously reported corresponding QTL with a 9.52–16.33% PVE was detected in both the 2013 and 2014 environments (Yu et al. 2019). Both of *qAftA07* and *qAftB06.2* were identified in five different environments, suggests their stability in conferring peanut resistance to aflatoxin production.

Due to the utilization of SSR markers for genetic map construction, the precise physical locations of the two major QTLs were undetermined in the previous study. The new genetic linkage map was constructed using the resequencing data of RILs, encompassing 2700 bin blocks (Li et al. 2023). With the new map, the *qAftA07* was precisely mapped to the genomic region spanning from 0.00 Mb to 3.60 Mb on the A07 chromosome (Table 2), which displayed an overlap with the major QTL *qAFTRA07.1* for AP resistance. The genomic region of *qAFTRA07.1*, spanning from 0.42 Mb to 0.52 Mb, was identified using a RIL population built by crossing of Xuhua 13 and Zhonghua 6. The gene *Arahy.K5EKT0* was recognized as a candidate gene, as a 54 bp deletion and four SNPs were detected within the second exon in the resistant parent Zhonghua 6 (Yu et al. 2024). However, no genetic variation was detected within the exons of *Arahy.K5EKT0*, whereas two SNPs were identified downstream of it. Additionally, no significantly difference in the expression level of *Arahy.K5EKT0* was observed between Zhonghua 10 and ICG 12625 after inoculated with *A. flavus* (Fig. S4A). Hence, the AP resistance in ICG 12625 was not attributed to functional loss of *Arahy.K5EKT0*, indicating that the resistant mechanism in ICG 12625 may differ from that observed in Zhonghua 6.

The genomic region of *qAftB06.2* was precisely mapped to the interval from 9.24 Mb to 21.75 Mb on the B06 chromosome using the new genetic map (Table 2). Three QTLs associated with peanut AP resistance were also identified on the B06 chromosome using a RIL population generated from the cross between Zhonghua 16 and J11. Unfortunately, the physical region of them were not reported (Jin et al. 2023).

The QTLs *qAftA01* and *qAftA10* were not detected in the previous study using SSR markers and have not been reported by other researchers, represent new genetic loci

associated with peanut AP resistance. However, they were only identified under specific environmental conditions (Table 2).

### The immune response in ICG 12625 displays a more robust and rapid reaction to infection of *A. flavus*

In this study, transcriptome analysis was performed on two parental lines inoculated with *A. flavus* to elucidate the molecular mechanisms underlying AP resistance and identify potential candidate genes conferring resistance. The RNA-seq data was collected at 0, 0.5, 1, 3 and 7 DAI, however, the alignment rates at 7 DAI only reached to 7.20–14.84% (Table S1). The same phenomenon was observed in the transcriptome analysis of peanut seeds from J11 and Zhonghua 12, which were inoculated with *A. flavus*. The average mapping genome ratios of Zhonghua 12 at 5 DAI and 7 DAI were only 23.12% and 17.27%, respectively (Cui et al. 2022). The seeds surface at 7 DAI were almost covered by green sporulation, leading to a predominant mapping of reads from samples collected at 7 DAI to the *A. flavus* genome.

In the resistant parent ICG 12615, a total of 18,161 genes were induced within the initial half-day after inoculated with *A. flavus*, whereas only 6213 genes were induced in Zhonghua 10 during that period (Fig. S1B). Subsequently, during the following half-day period, only 3408 genes were regulated in ICG 12625, while a larger set of 4630 genes were regulated in Zhonghua 10 (Fig. S1B). Then, over the course of the subsequent two days, ICG 12625 showed regulation in just 3408 genes while Zhonghua 10 exhibited regulation in a higher number of genes (7241) (Fig. S1B). The number of induced genes was comparable between ICG 12625 and Zhonghua 10 (55,188 vs. 53,476) (Fig. S1A). However, a sharp increase in induced genes was observed in the first half-day after inoculation with *A. flavus* in ICG 12625, whereas the induction of genes remained relatively mild throughout the entire infection process of *A. flavus* in Zhonghua 10. Therefore, the immune response to *A. flavus* infection is more robust and rapid in ICG 12625, while it is milder in Zhonghua 10.

Although the response speed to *A. flavus* infection differs between in ICG 12625 and Zhonghua 10, the KEGG pathways involved in the response to *A. flavus* infection are similar. A total of 123 pathways were significantly enriched throughout the entire infection process in both of Zhonghua 10 and ICG 12625 (Fig. S1F), including plant hormone signal transduction, plant-pathogen interaction, oxidative phosphorylation, flavonoid biosynthesis, isoflavonoid biosynthesis, phenylpropanoid biosynthesis, sulfur metabolism, glutathione metabolism and alpha-linolenic acid metabolism (Fig. 2C). These pathways have also been reported to be participated in the response to *A. flavus* infection by other

researchers (Cui et al. 2022; Soni et al. 2020b, 2021; Wang et al. 2016). Hence, the pathways implicated in peanut resistance against AP are largely conserved. The difference between ICG 12625 and Zhonghua 10 lies in the higher number of induced genes observed in ICG 12625, as well as a more pronounced fold-change.

### The predicted candidate genes show higher priorities in identification of resistance genes

The WGCNA analysis facilitates the extraction of pertinent genes from phenotype data and is extensively employed for investigating intricate relationships among different gene types (Yu et al. 2023). It has been used in peanut to identify hub genes associated with resistance to *A. flavus*. As a result, 18 genes encoding pathogenesis-related proteins, 1-aminocyclopropane-1-carboxylate oxidase, MAPK kinase, serine/threonine kinase, pattern recognition receptors, cytochrome P450, SNARE protein SYP121, pectinesterase, phosphatidylinositol transfer protein, and pentatricopeptide repeat protein were characterized as hub genes in peanut resistance to *A. flavus* (Cui et al. 2022). The WGCNA approach has also been widely employed in candidate gene prediction in maize, wheat and soybean (Ma et al. 2021; Wei et al. 2022; Zhao et al. 2024b). It has been successfully used in peanut to identify a potential candidate gene associated with sucrose content, exhibiting a significant negative correlation between its expression level and sucrose content (Huai et al. 2024). Therefore, the WGCNA can be utilized to identify and prioritize potential candidate genes.

In this study, the WGCNA was used to predict potential candidate genes associated with peanut AP resistance in *qAftA07* and *qAftB06.2*. Four modules exhibited a significant correlation with aflatoxin content in seeds from Zhonghua 10 and ICG 12625 (Fig. 3B). In the candidate region of *qAftA07* and *qAftB06.2*, 10 and 11 genes from these modules were respectively identified as highly promising candidate genes (Table 5). The candidate gene *Arahy.VX6XNZ* encodes a predicted NUDIX hydrolase, which has been reported to be involved in the regulation of biotic stress responses in *Arabidopsis* (Yoshimura and Shigeoka 2015). The candidate gene *Arahy.VV0UJ5* encodes a member cytochrome P450 family, which are one of the main enzymes in charge of detoxifying exogenous molecules in plants. When pathogens attack host plants, cytochrome P450 enzymes respond by inhibiting the formation of antibiotic phytoalexins (Chakraborty et al. 2023). The candidate gene *Arahy.706LQI* encodes a calcium-dependent protein kinase, which belongs to the plant-specific family of calcium receptor and kinase effector proteins. Calcium-dependent protein kinases play a crucial role in plant defense against pathogens by sensing fluctuations in intracellular calcium ion levels, transducing signals to downstream immune-related molecules, and

initiating a cascade of defense responses encompassing the synthesis of antibacterial compounds, reinforcement of the cell wall, and regulation of programmed cell death (Schulz et al. 2013). The candidate gene *Arahy.A6JL9Q* encodes a bifunctional 3-dehydroquinate dehydratase/shikimate dehydrogenase (DHQ-SDH), which plays a crucial role in the shikimic acid pathway. It serves to regulate the utilization of intermediates within the competitive pathway, thereby increasing metabolite circulation efficiency. Upon pathogen infection, the DHQ-SDH enzyme promptly modulates shikimic acid metabolism, facilitating augmented synthesis of defense-related compounds and enhancing plant resistance (Huang et al. 2019). The candidate gene *Arahy.C6NV9N* encodes a GATA transcription factor, potentially participate in the plant hormone signal transduction and exerting influence on plant defense (Richter et al. 2013). The candidate gene *Arahy.6QIKS5* encodes a S-adenosylmethionine synthase, which was reported to be involved in lignin biosynthesis in switchgrass (Li et al. 2022). The candidate gene *Arahy.1G1J9V* encodes a dormancy-associated protein (DRM), exhibiting a comparatively lower expression level in ICG 12625 compared to Zhonghua 10 (Fig. 3D). Over expression of *OsDRM1* gene in rice prolonged the dormancy period (Chen et al. 2023). This suggests that the dormancy period of ICG12625 may be shorter and more susceptible to induction by infection of *A. flavus*. Consequently, the predicted candidate genes show higher priorities for further analysis of peanut AP resistance-associated resistance genes.

Although the most promising candidate genes for *qAftA07* and *qAftB06.2* were identified, their specific functions and contributions to aflatoxin resistance still require verification. Revealing the impacts of knocking-out or over-expressing these candidate genes in peanut on aflatoxin resistance is imperative for comprehensive understanding. The candidate QTLs and genes should also be assessed for their broad applicability by introducing them into diverse genetic backgrounds of peanut varieties and subjecting them to a wider range of environmental conditions. Furthermore, the integration of multi-omics data encompassing proteomics and metabolomics would facilitate a more comprehensive analysis of the candidate genes.

## Conclusion

The present study identified two major QTLs, *qAftA07* and *qAftB06.2*, associated with peanut AP resistance with 6.83–16.52% PVE. Transcriptome analysis revealed a more robust and rapid immune response in ICG 12625 upon infection with *A. flavus*, as compared to that observed in Zhonghua 10. By integrating the WGCNA results with the candidate regions of major QTLs, 10 and 11 genes were respectively identified in *qAftA07* and *qAftB06.2*, which

showed a strong correlation with aflatoxin content. These predicted candidate genes were considered as the most promising candidate genes within these two QTLs. Additionally, this study provides valuable insights for future map-based cloning studies targeting candidate genes associated with AP resistance in peanut.

**Supplementary Information** The online version contains supplementary material available at <https://doi.org/10.1007/s00122-025-04822-1>.

**Author contribution statement** DH, LH, YL and BL conceived and designed the experiments; HJ and LH supplied the peanut population; XX, BY, YD, GJ, HL, XZ, NL, WC, YC, XW, QW, YK and ZW performed the experiments; DH, LH, XX and HL analyzed the data; DH and HL wrote the manuscript; DH, LH, MKP, HKS, XC, YL and BL contributed in data interpretation and revision of the manuscript. All authors have read and approved the final version of the manuscript.

**Funding** This work was supported by the National Natural Science Foundation of China (32001510, 32101708, 31461143022 and 32161143006), the National Peanut Industry Technology System Construction (CARS-13), the Key R&D Program of China (2022YFD1200400 and 2023YFD1202800) and Innovation Program of the Chinese Academy of Agricultural Sciences (2024-2060299-089-031). The funders had no role in experiment design, data analysis, decision to publish, or preparation of the manuscript.

**Data availability** The datasets presented in this study can be found in online repositories. The names of the repository/repositories and accession number(s) can be found below: <https://ngdc.cncb.ac.cn/bioproject/>, PRJCA028982.

## Declarations

**Conflict of interest** The authors declare that they have no conflict of interest.

## References

- Alameri MM, Kong AS-Y, Aljaafari MN, Ali HA, Eid K, Sallagi MA, Cheng W-H, Abushelaibi A, Lim S-HE, Loh J-Y (2023) Aflatoxin contamination: an overview on health issues, detection and management strategies. *Toxins* 15:246
- Basten CJ, Weir BS, Zeng ZB (2002) QTL Cartographer, version 1.17. Department of Statistics, North Carolina State University, Raleigh
- Bertioli DJ, Jenkins J, Clevenger J, Dudchenko O, Gao D, Seijo G, Leal-Bertioli SC, Ren L, Farmer AD, Pandey MK (2019) The genome sequence of segmental allotetraploid peanut *Arachis hypogaea*. *Nat Genet* 1:66
- Bhatnagar-Mathur P, Yogendra K, Parankusam S, Sanivarapu H, Prasad K, Lingampali SB, Sharma KK (2021) Comparative proteomics provide insights on the basis of resistance to *Aspergillus flavus* infection and aflatoxin production in peanut (*Arachis hypogaea* L.). *J Plant Interact* 16:494–509
- Bolger AM, Lohse M, Usadel B (2014) Trimmomatic: a flexible trimmer for Illumina sequence data. *Bioinformatics* 30:2114–2120
- Chai P, Cui M, Zhao Q, Chen L, Guo T, Guo J, Wu C, Du P, Liu H, Xu J (2024) Genome-wide characterization of the phenylalanine ammonia-lyase gene family and their potential roles in response to *Aspergillus flavus* L. infection in cultivated peanut (*Arachis hypogaea* L.). *Genes* 15:265
- Chakraborty P, Biswas A, Dey S, Bhattacharjee T, Chakrabarty S (2023) Cytochrome P450 gene families: role in plant secondary metabolites production and plant defense. *J Xenobiot* 13:402–423
- Chen C, Chen H, Zhang Y, Thomas HR, Frank MH, He Y, Xia R (2020) TBtools: an integrative toolkit developed for interactive analyses of big biological data. *Mol Plant* 13:1194–1202
- Chen R, Luo L, Li K, Li Q, Li W, Wang X (2023) Dormancy-associated gene 1 (OsDRM1) as an axillary bud dormancy marker: retarding plant development, and modulating auxin response in rice (*Oryza sativa* L.). *J Plant Physiol* 291:154117
- Cingolani P, Platts A, Wang LL, Coon M, Nguyen T, Wang L, Land SJ, Lu X, Ruden DM (2012) A program for annotating and predicting the effects of single nucleotide polymorphisms, SnpEff: SNPs in the genome of *Drosophila melanogaster* strain w1118; iso-2; iso-3. *fly* 6:80–92
- Consortium GO (2019) The gene ontology resource: 20 years and still GOing strong. *Nucleic Acids Res* 47:D330–D338
- Cui M, Han S, Wang D, Haider MS, Guo J, Zhao Q, Du P, Sun Z, Qi F, Zheng Z (2022) Gene co-expression network analysis of the comparative transcriptome identifies hub genes associated with resistance to *Aspergillus flavus* L. in cultivated peanut (*Arachis hypogaea* L.). *Front Plant Sci* 13:899177
- Ding Y, Qiu X, Luo H, Huang L, Guo J, Yu B, Sudini H, Pandey M, Kang Y, Liu N (2022) Comprehensive evaluation of Chinese peanut mini-mini core collection and QTL mapping for aflatoxin resistance. *BMC Plant Biol* 22:207
- Feng C, Sun Z, Zhang L, Feng L, Zheng J, Bai W, Gu C, Wang Q, Xu Z, van der Werf W (2021) Maize/peanut intercropping increases land productivity: a meta-analysis. *Field Crops Res* 270:108208
- Huai D, Zhi C, Wu J, Xue X, Hu M, Zhang J, Liu N, Huang L, Yan L, Chen Y (2024) Unveiling the molecular regulatory mechanisms underlying sucrose accumulation and oil reduction in peanut kernels through genetic mapping and transcriptome analysis. *Plant Physiol Biochem* 208:108448
- Huang K, Li M, Liu Y, Zhu M, Zhao G, Zhou Y, Zhang L, Wu Y, Dai X, Xia T (2019) Functional analysis of 3-dehydroquinase dehydratase/shikimate dehydrogenases involved in shikimate pathway in *Camellia sinensis*. *Front Plant Sci* 10:1268
- Jallow A, Xie H, Tang X, Qi Z, Li P (2021) Worldwide aflatoxin contamination of agricultural products and foods: from occurrence to control. *Compr Rev Food Sci Food Saf* 20:2332–2381
- Jiang Y, Luo H, Yu B, Ding Y, Kang Y, Huang L, Zhou X, Liu N, Chen W, Guo J (2021) High-density genetic linkage map construction using whole-genome resequencing for mapping QTLs of resistance to *Aspergillus flavus* infection in peanut. *Front Plant Sci* 12:745408
- Jin G, Liu N, Yu B, Jiang Y, Luo H, Huang L, Zhou X, Yan L, Kang Y, Huai D (2023) Identification and pyramiding major QTL loci for simultaneously enhancing aflatoxin resistance and yield components in peanut. *Genes* 14:625
- Kanehisa M, Furumichi M, Tanabe M, Sato Y, Morishima K (2017) KEGG: new perspectives on genomes, pathways, diseases and drugs. *Nucleic Acids Res* 45:D353–D361
- Khan SA, Chen H, Deng Y, Chen Y, Zhang C, Cai T, Ali N, Mamadou G, Xie D, Guo B (2020) High-density SNP map facilitates fine mapping of QTLs and candidate genes discovery for *Aspergillus flavus* resistance in peanut (*Arachis hypogaea*). *Theor Appl Genet* 133:2239–2257
- Kim D, Paggi JM, Park C, Bennett C, Salzberg SL (2019) Graph-based genome alignment and genotyping with HISAT2 and HISAT-genotype. *Nat Biotechnol* 37:907–915
- Langfelder P, Horvath S (2008) WGCNA: an R package for weighted correlation network analysis, vol 9, pp 1–13
- Li B, Dewey CN (2011) RSEM: accurate transcript quantification from RNA-Seq data with or without a reference genome. *BMC Bioinform* 12:1–16

- Li Y, Xiong W, He F, Qi T, Sun Z, Liu Y, Bai S, Wang H, Wu Z, Fu C (2022) Down-regulation of *PvSAMS* impairs S-adenosyl-L-methionine and lignin biosynthesis, and improves cell wall digestibility in switchgrass. *J Exp Bot* 73:4157–4169
- Li W, Huang L, Liu N, Chen Y, Guo J, Yu B, Luo H, Zhou X, Huai D, Chen W (2023) Identification of a stable major sucrose-related QTL and diagnostic marker for flavor improvement in peanut. *Theor Appl Genet* 136:78
- Love MI, Huber W, Anders S (2014) Moderated estimation of fold change and dispersion for RNA-seq data with DESeq2. *Genome Biol* 15:1–21
- Ma L, Zhang M, Chen J, Qing C, He S, Zou C, Yuan G, Yang C, Peng H, Pan G (2021) GWAS and WGCNA uncover hub genes controlling salt tolerance in maize (*Zea mays* L.) seedlings. *Theor Appl Genet* 134:3305–3318
- Mingrou L, Guo S, Ho CT, Bai N (2022) Review on chemical compositions and biological activities of peanut (*Arachis hypogaea* L.). *J Food Biochem* 46:e14119
- Richter R, Behringer C, Zourelidou M, Schwechheimer C (2013) Convergence of auxin and gibberellin signaling on the regulation of the GATA transcription factors GNC and GNL in *Arabidopsis thaliana*. *Proc Natl Acad Sci* 110:13192–13197
- Schulz P, Herde M, Romeis T (2013) Calcium-dependent protein kinases: hubs in plant stress signaling and development. *Plant Physiol* 163:523–530
- Shabeer S, Asad S, Jamal A, Ali A (2022) Aflatoxin contamination, its impact and management strategies: an updated review. *Toxins* 14:307
- Sharma S, Choudhary B, Yadav S, Mishra A, Mishra VK, Chand R, Chen C, Pandey SP (2021) Metabolite profiling identified piperolic acid as an important component of peanut seed resistance against *Aspergillus flavus* infection. *J Hazard Mater* 404:124155
- Soni P, Nayak SN, Kumar R, Pandey MK, Singh N, Sudini HK, Bajaj P, Fountain JC, Singam P, Hong Y (2020b) Transcriptome analysis identified coordinated control of key pathways regulating cellular physiology and metabolism upon *Aspergillus flavus* infection resulting in reduced aflatoxin production in groundnut. *J Fungi* 6:370
- Soni P, Pandey AK, Nayak SN, Pandey MK, Tolani P, Pandey S, Sudini HK, Bajaj P, Fountain JC, Singam P (2021) Global transcriptome profiling identified transcription factors, biological process, and associated pathways for pre-harvest aflatoxin contamination in groundnut. *J Fungi* 7:413
- Soni P, Gangurde SS, Ortega-Beltran A, Kumar R, Parmar S, Sudini HK, Lei Y, Ni X, Huai D, Fountain JC (2020) Functional biology and molecular mechanisms of host-pathogen interactions for aflatoxin contamination in groundnut (*Arachis hypogaea* L.) and maize (*Zea mays* L.). *Front Microbiol* 11:227
- Thimm O, Bläsing O, Gibon Y, Nagel A, Meyer S, Krüger P, Selbig J, Müller LA, Rhee SY, Stitt M (2004) MAPMAN: a user-driven tool to display genomics data sets onto diagrams of metabolic pathways and other biological processes. *Plant J* 37:914–939
- Torres AM, Barros GG, Palacios SA, Chulze SN, Battilani P (2014) Review on pre- and post-harvest management of peanuts to minimize aflatoxin contamination. *Food Res Int* 62:11–19
- Wang H, Lei Y, Wan L, Yan L, Lv J, Dai X, Ren X, Guo W, Jiang H, Liao B (2016) Comparative transcript profiling of resistant and susceptible peanut post-harvest seeds in response to aflatoxin production by *Aspergillus flavus*. *BMC Plant Biol* 16:1–16
- Wang Y, Liu D, Yin H, Wang H, Cao C, Wang J, Zheng J, Liu J (2023) Transcriptomic and metabolomic analyses of the response of resistant peanut seeds to *Aspergillus flavus* infection. *Toxins* 15:414
- Wei J, Fang Y, Jiang H, Wu X-t, Zuo J-h, Xia X-c, Li J-q, Stich B, Cao H, Liu Y-x (2022) Combining QTL mapping and gene co-expression network analysis for prediction of candidate genes and molecular network related to yield in wheat. *BMC Plant Biol* 22:288
- Yoshimura K, Shigeoka S (2015) Versatile physiological functions of the Nudix hydrolase family in Arabidopsis. *Biosci Biotechnol Biochem* 79:354–366
- Yu B, Huai D, Huang L, Kang Y, Ren X, Chen Y, Zhou X, Luo H, Liu N, Chen W (2019) Identification of genomic regions and diagnostic markers for resistance to aflatoxin contamination in peanut (*Arachis hypogaea* L.). *BMC Genet* 20:1–13
- Yu B, Jiang H, Pandey MK, Huang L, Huai D, Zhou X, Kang Y, Varshney RK, Sudini HK, Ren X (2020) Identification of two novel peanut genotypes resistant to aflatoxin production and their SNP markers associated with resistance. *Toxins* 12:156
- Yu J, Zhu C, Xuan W, An H, Tian Y, Wang B, Chi W, Chen G, Ge Y, Li J (2023) Genome-wide association studies identify *OsWRKY53* as a key regulator of salt tolerance in rice. *Nat Commun* 14:3550
- Yu B, Liu N, Huang L, Luo H, Zhou X, Lei Y, Yan L, Wang X, Chen W, Kang Y (2024) Identification and application of a candidate gene *AhAfr1* for aflatoxin production resistance in peanut seed (*Arachis hypogaea* L.). *J Adv Res* 62:15–26
- Zhao X, Zhang Y, Wang J, Zhao X, Li Y, Teng W, Han Y, Zhan Y (2024b) GWAS and WGCNA analysis uncover candidate genes associated with oil content in soybean. *Plants* 13:1351
- Zhao Q, Cui M, Guo T, Shi L, Qi F, Sun Z, Du P, Liu H, Zhang Y, Zheng Z (2024a) Genome-wide characterization and expression analysis of the cultivated peanut *AhPR10* gene family mediating resistance to *Aspergillus flavus* L. *J Integr Agric*

**Publisher's Note** Springer Nature remains neutral with regard to jurisdictional claims in published maps and institutional affiliations.

Springer Nature or its licensor (e.g. a society or other partner) holds exclusive rights to this article under a publishing agreement with the author(s) or other rightsholder(s); author self-archiving of the accepted manuscript version of this article is solely governed by the terms of such publishing agreement and applicable law.